

SKINNING DURING DESORPTION OF POLYMERS: AN ASYMPTOTIC ANALYSIS*

D. A. EDWARDS†

Abstract. Desorption of saturated polymers can be inhibited if a nearly dry (glassy) skin with a low diffusion coefficient forms at the exposed surface. In addition, trapping skinning can occur, where an increase in the force driving the desorption decreases the accumulated flux desorbed. The dynamics of such systems cannot be described by the simple Fickian diffusion equation. The mathematical model presented is a moving boundary-value problem with a set of two coupled partial differential equations. Most previous studies of this model focused on sorption studies; this is the first that considers desorption into an environment of arbitrary concentration. Since the derived equations cannot be solved by similarity variables, integral equation techniques are used to obtain asymptotic estimates for the solution. The skinning solution obtained also exhibits fronts moving with constant speed, another distinctive feature of non-Fickian polymer-penetrant systems.

Key words. asymptotic expansions, desorption, moving boundary-value problems, perturbation methods, polymer-penetrant systems, skinning

AMS subject classifications. 35B20, 35C15, 35C20, 35K60, 35R35, 73F15, 76R99, 80A22

PII. S0036139996311060

1. Introduction. Due to their wide applicability, much experimental and theoretical work has been devoted to the study of polymer-penetrant systems over the past few decades. One unusual yet industrially exploitable feature of such systems is a change of state in the polymer from a *rubbery* state (denoted by sub- and superscript r) when it is nearly saturated to a *glassy* state (denoted by sub- and superscript g) when it is nearly dry. Sometimes a glassy region develops at the exposed surface when a saturated polymer film or fiber is desorbed. This region, which is often thin for films of finite thickness, is called a *glassy skin*. Since the polymer is now in two states—the glassy skin and the deeper rubbery material—this phenomenon is called *literal skinning* [1], [2], [3].

This glassy skin can be exploited for the production of more effective protective clothing, equipment, or sealants from polymer materials [4], [5], [6]. In addition, the skin may slow desorption of saturated films because the diffusion coefficient in the glassy region is much lower than in the rubbery region [7]. Such slowing can be useful in spray drying operations [8] or membrane production by phase inversion [9]. However, polymer skinning is undesirable in coating processes due to a decrease in the drying rates and the formation of nonuniformities in the polymer coating [3].

When certain polymer-penetrant systems are desorbed, a glassy skin may develop such that an even more unusual phenomenon, called *trapping skinning*, can occur. Normally, an increase in the driving force for the desorption will increase the accumulated flux through the exposed surface. However, in trapping skinning an increase in the force driving the desorption *decreases* the accumulated flux! To describe this behavior, effects other than the lower diffusion coefficient in the skin must be included [2], [3], [10].

*Received by the editors October 25, 1996; accepted for publication (in revised form) May 9, 1998; published electronically March 23, 1999. This research was supported by National Science Foundation grant DMS-9407531.

<http://www.siam.org/journals/siap/59-3/31106.html>

†Department of Mathematics, Mathematics Building 084, University of Maryland, College Park, MD 20742-4015. Present address: Department of Mathematical Sciences, University of Delaware, Newark, DE 19716-2553 (edwards@math.udel.edu).

Although all the physical mechanisms for these phenomena are not known, most scientists agree that one important factor is a viscoelastic stress in the polymer entanglement network. This stress, which is a nonlinear memory effect, depends on the *relaxation time*, which measures the time necessary for the polymer entanglement network to react to nonlocal changes in concentration. In many polymer-penetrant systems, the stress is as important to the transport process as the well-understood Fickian dynamics [11], [12], [13]. In the glassy skin the relaxation time is finite, so the stress is an important effect. However, in the rubbery region the memory effect is not as important because the relaxation time is nearly zero [5], [11], [14].

A set of model equations for general polymer-penetrant systems of this type has been derived in detail by Edwards and Cohen [15], [16]. The model consists of a set of coupled partial differential equations. Various parameters in the problem are considered to have discontinuously different values in the two states. Therefore a moving boundary-value problem that cannot be solved by similarity solutions ensues. However, some results can be obtained using asymptotic and singular perturbation techniques.

Previous studies of this model have been concerned almost exclusively with the important problem of sorption experiments, including case II diffusion and the failure of polymer films [15], [16], [17], [18], [19]. Due to the viscoelastic memory of the polymer, desorption studies cannot be considered from a mathematical point of view as simple reversals of the sorption process. Therefore, these previous studies are of limited utility for the system at hand. One study of desorption has used this model [20], but it suffers because the results therein, which hold for desorption into a dry environment, cannot be extended to the case of so-called “humid” environments, where the concentration of the penetrant in the environment is nonzero. In this work, we present results which are applicable to both dry and “humid” environments.

When modeling the desorption process, two physical quantities are of interest: the accumulated flux through the boundary and the motion of the glass-rubber interface. In this work, we provide descriptions of each of these quantities in terms of dimensionless parameters in our problem. These descriptions should provide useful data to chemical engineers who wish to verify our model experimentally and, if our model is shown to be accurate, to those who wish to design new products that exploit the skinning phenomenon.

2. Governing equations. We wish to study the following dimensionless model for anomalous diffusion in polymers:

$$(2.1a) \quad C_t = [D(C)C_x + \sigma_x]_x, \quad x > 0, \quad t > 0,$$

$$(2.1b) \quad \sigma_t + \frac{\beta(C)}{\beta_g} \sigma = \frac{\mu}{\nu\beta_g} C + C_t,$$

$$(2.2) \quad \beta(C) = \begin{cases} \beta_g, & 0 \leq C \leq C_* \quad (\text{glass}), \\ \beta_r, & C_* < C \leq 1 \quad (\text{rubber}), \end{cases}$$

$$(2.3) \quad D(C) = \begin{cases} D_g, & 0 \leq C \leq C_*, \\ D_r, & C_* \leq C \leq 1, \end{cases}$$

where C is the concentration of the penetrant, $D(C)$ is the molecular diffusion coefficient, $\beta(C)$ is the inverse of the relaxation time, C_* is the glass-rubber transition concentration, and μ and ν are positive constants. Various forms quite similar to (2.1) have been used successfully to model many types of anomalous behavior in polymer-penetrant systems [15], [17], [18], [19], [20]. Although (2.1a) and (2.1b) are derived in detail in [20], a brief summary is appropriate here.

Given the general form of the diffusion equation $C_t = -J_x$, where J is the flux, we see that the flux in (2.1a) has been augmented by a term which depends on the nonstate variable σ . Such a term can be obtained by postulating that the chemical potential is a function of both C and σ [15]. Since the evolution equation (2.1b) for σ is reminiscent of the one for viscoelastic stress, we refer to σ , which models the effects of polymer memory, as a “stress” throughout this work. However, it should be considered as the stress for the polymer network rather than the total stress in the system.

By modeling the polymer as a semi-infinite slab, we are able to neglect shrinking of the polymer matrix as it is desorbed [3]. However, we expect the effects of such shrinkage to manifest themselves through a negative (compressive) stress. In (2.1a) and (2.1b) we have normalized C by the saturation concentration. In addition, we use the relaxation time in the glassy polymer as a time scale since it is on the order of seconds and hence physically observable. We also choose a physically observable length scale associated with the stress.

To obtain a system which is amenable to asymptotic techniques, we have taken $D(C)$ and $\beta(C)$ to be piecewise constant. However, this simplification is justifiable physically. In many polymer-penetrant systems, both $\beta(C)$ and $D(C)$ increase dramatically as the polymer goes from the glassy to the rubbery state [5], [11], [14], [21], [22]. In contrast, the differences in these parameters *within* states are qualitatively negligible when compared with the differences *between* states. Hence we replace $\beta(C)$ and $D(C)$ by their averages in each state, yielding (2.2) and (2.3). Crank [23] used such a piecewise-constant form for $D(C)$ to study these anomalous systems. Cohen and White [24] discuss various other physically appropriate forms for these parameters.

We model the desorption of a polymer which is initially saturated; the correct dimensionless boundary and initial conditions are given by [20]

$$(2.4a) \quad C(x, 0) = 1,$$

$$(2.4b) \quad \sigma(x, 0) = \sigma_i(x),$$

$$(2.5) \quad D(C)C_x(0, t) + \sigma_x(0, t) = k[C(0, t) - C_{\text{ext}}],$$

where C_{ext} is the concentration of the penetrant in the external environment and k is a constant measuring the permeability of the exposed boundary. We have left (2.4b) arbitrary for now; discussion of the proper condition to impose is postponed until section 3. Equation (2.5), which is a radiation condition, states that the flux out of the polymer is proportional to the difference between the surface and exterior concentrations. Edwards [20] examined diffusion only into dry environments where $C_{\text{ext}} = 0$. Due to the nonlinear nature of (2.1a) and (2.1b), a simple shift $C \mapsto C - C_{\text{ext}}$ does not yield another solution to the problem. Unfortunately, due to the sizes of the parameters studied in [20], the results therein are not applicable for

“humid” environments where $C_{\text{ext}} \neq 0$. In this work we model both “humid” and dry environments by allowing C_{ext} to be arbitrary. Last, we expect that as time progresses the polymer will approach equilibrium with the outside environment, so we have

$$(2.6) \quad C(x, \infty) = C_{\text{ext}}.$$

Our problem will involve matching the solutions of our equations in the two regions where $\beta = \beta_g$ and $\beta = \beta_r$. Thus, it is necessary to impose conditions at the moving boundary $x = s(t)$ separating the two regions. These are given by [20]

$$(2.7) \quad C^r(s(t), t) = C_* = C^g(s(t), t),$$

$$(2.8) \quad \sigma^r(s(t), t) = \sigma^g(s(t), t),$$

$$(2.9) \quad [D(C)C_x + \sigma_x]_s = a\dot{s},$$

where a , the *change-of-state* parameter, is a constant, the dot indicates differentiation with respect to t , and we have defined the operator $[f]_s \equiv f^g(s^-(t), t) - f^r(s^+(t), t)$. As indicated above, the glass-rubber interface $x = s(t)$ is defined to be that curve at which $C = C_*$. Therefore, we have no jump in concentration at that point and (2.7) results. In (2.8) we postulate that the stress will also be continuous at $x = s(t)$, although other researchers do not [25]. Instead, we expect that differences in the polymer network stress evolution in each region will manifest themselves through a discontinuous stress gradient, as seen in (2.9), which is directly analogous to the phase-change condition in a standard two-phase heat conduction problem. This reflects the stretching or swelling of the polymer as it changes from glass to rubber. The flux used up in this stretching is directly analogous to the energy used up in melting, and so we use the condition that the difference between the flux in and out of the front is proportional to its speed.

Since $\beta(C)$ and $D(C)$ are piecewise constant, (2.1a) can be rewritten as

$$(2.10) \quad C_t = D(C)C_{xx} + \sigma_{xx}.$$

Combining (2.10) and (2.1b) yields

$$(2.11) \quad C_{tt} = [1 + D(C)]C_{xxt} - \frac{\beta(C)}{\beta_g}C_t + \left[\frac{\beta(C)D(C)}{\beta_g} + \frac{\mu}{\nu\beta_g} \right] C_{xx}.$$

It can be shown that (2.11) also holds for σ .

In addition, if one solves (2.1b) for σ and uses the results in (2.9), it can be shown [16] that the front condition (2.9) is equivalent to

$$(2.12) \quad [(D(C) + 1)C_x]_s + \left(1 - \frac{\beta_r}{\beta_g} \right) \frac{\sigma(s(t), t)}{\dot{s}} = a\dot{s}.$$

The presence of \dot{s} in the denominator of the second term on the left-hand side of (2.12) is highly nonstandard. Due to the presence of this term, a standard similarity-solution approach is fruitless.

Since we wish to use a perturbation approach to solve our equations, we must examine the relative size of our parameters. Experimentally it has been shown that polymers have an infinitesimal relaxation time in the rubbery state, while in the

glassy state these substances are characterized by finite relaxation times. Hence we let $\beta_g/\beta_r = \epsilon$, where $0 < \epsilon \ll 1$, and use this as our perturbation parameter.

It also has been shown experimentally that the diffusion coefficient is much smaller in the glassy state than in the rubbery state, so we set $D_g = D_0\epsilon$. This small diffusion coefficient can inhibit the desorption process if a glassy skin forms. Since D_g is so small, the dominant contribution to the flux in the glassy region is given by the stress term. This agrees with the observation that nonlinear relaxation effects are most pronounced in the glassy region.

Since the polymer network shrinks as it dries, we expect a negative (compressive) stress in the glassy region. The C_t term in (2.1b) is negative, while μ is positive. Therefore, we may obtain a negative stress if we allow the C_t term to dominate by setting $\mu = \mu_0\epsilon$. We wish to examine highly permeable polymers, so we let $k = k_0\epsilon^{-1}$. Last, for reasons which will become clear later, we require that

$$(2.13) \quad a > C_* - 1.$$

Since a can be negative, we see that the strict analogy to a Stefan problem is inaccurate. However, a negative a can still yield results which are physically realistic [15]. We also note that $a = 0$ is allowed under (2.13). This value for a corresponds to a continuous flux across the interface, which some authors prefer to the front condition (2.9).

Substituting these values for our parameters into (2.11) and (2.1b) in the glassy region, we obtain

$$(2.14a) \quad C_{tt}^g = (1 + D_0\epsilon)C_{xxt}^g - C_t^g + \epsilon(D_0 + \gamma)C_{xx}^g, \quad \gamma = \frac{\mu_0}{\nu\beta_g},$$

$$(2.14b) \quad \sigma_t^g + \sigma^g = \gamma\epsilon C^g + C_t^g.$$

Since (2.11) also holds for σ , we see from (2.14a) that we have the following equation for the polymer network stress in the glassy region:

$$(2.15) \quad \sigma_{tt}^g = (1 + D_0\epsilon)\sigma_{xxt}^g - \sigma_t^g + \epsilon(D_0 + \gamma)\sigma_{xx}^g.$$

Using our values for the parameters in the rubbery region, we have

$$(2.16a) \quad C_{tt}^r = \alpha C_{xxt}^r - \frac{1}{\epsilon}C_t^r + \left(\frac{D_r}{\epsilon} + \gamma\epsilon\right)C_{xx}^r, \quad \alpha = 1 + D_r,$$

$$(2.16b) \quad \sigma_t^r + \frac{1}{\epsilon}\sigma^r = \gamma\epsilon C^r + C_t^r.$$

In addition, (2.12) can be written as

$$(2.17) \quad (D_0\epsilon + 1)C_x^g(s(t), t) - \alpha C_x^r(s(t), t) + \left(1 - \frac{1}{\epsilon}\right)\frac{\sigma(s(t), t)}{\dot{s}} = a\dot{s}.$$

If the outer boundary is in the rubbery region, (2.5) becomes

$$(2.18a) \quad D_r C_x^r(0, t) + \sigma_x^r(0, t) = k_0\epsilon^{-1}[C^r(0, t) - C_{\text{ext}}],$$

while if it is in the glassy region we have

$$(2.18b) \quad D_0\epsilon C_x^g(0, t) + \sigma_x^g(0, t) = k_0\epsilon^{-1}[C^g(0, t) - C_{\text{ext}}].$$

3. The rubbery region. We postulate the following expansions in ϵ for the functions in the rubbery region:

$$(3.1) \quad C^r \sim C^{0r} + \epsilon C^{1r} + o(\epsilon), \quad \sigma^r \sim \sigma^{0r} + \epsilon \sigma^{1r} + o(\epsilon).$$

Then (2.16) and (2.4a) become, to leading orders,

$$(3.2a) \quad C_t^{0r} = D_r C_{xx}^{0r}, \quad x > s(t), \quad t > 0,$$

$$(3.2b) \quad \sigma_t^{0r} + \frac{1}{\epsilon}(\sigma^{0r} + \epsilon \sigma^{1r}) = \gamma \epsilon C^{0r} + C_t^{0r} + \epsilon C_t^{1r},$$

$$(3.3) \quad C^{0r}(x, 0) = 1.$$

As the experiment begins, we expect the entire polymer to be rubbery, so we must solve (3.2) subject to (2.18a). Matching the ϵ^{-1} terms in (3.2b), we have the following:

$$(3.4) \quad \sigma^{0r} \equiv 0.$$

Therefore, for consistency we should set $\sigma_i(x) = o(1)$. If instead we had imposed an $O(1)$ value for $\sigma_i(x)$, we would have to insert a thin initial layer where the stress would quickly decay to an $o(1)$ value. Such a layer is not of physical interest, and hence we shall use (3.4) as our solution and not consider any thin initial layer.

Substituting (3.4) into (2.18a), we obtain, to leading order,

$$(3.5) \quad C^{0r}(0, t) = C_{\text{ext}},$$

and we have two cases to consider. If $C_{\text{ext}} \geq C_*$, the exterior environment is so “humid” that if the polymer were ever in the glassy state, it would start absorbing penetrant from the environment. Therefore, the entire polymer is always rubbery and the solution is trivially obtained by solving (3.2a) subject to (3.3) and (3.5):

$$(3.6) \quad C^{0r}(x, t) = C_{\text{ext}} + (1 - C_{\text{ext}}) \operatorname{erf}\left(\frac{x}{2\sqrt{D_r t}}\right).$$

Now we consider the case where $C_{\text{ext}} < C_*$, in which case (3.5) is inconsistent with the definition of the rubbery region. Thus, the polymer must immediately develop a glassy skin at the boundary. This result is consistent with those in [20] in the limit that $k = O(\epsilon^{-1})$. Since there are two states in the polymer, we must solve the full moving boundary-value problem.

To obtain a solution, we first check if there can be an interior layer near the moving front. If we introduce an interior-layer variable about the moving front, the resulting operator has only solutions which grow exponentially as we exit the layer. Since these interior solutions cannot match to our solution away from the front, we see that such a layer cannot exist and the boundary condition at the front must be satisfied exactly. Indeed, since the same operator holds for C and σ , there also is no interior layer in σ , so from (3.4) we have that

$$(3.7) \quad \sigma^0(s(t), t) = 0.$$

To obtain another piece of information for use in (2.17), we solve for $\sigma^{1r}(s(t), t)$. Matching the $O(1)$ terms in (3.2b), we have the following at $x = s(t)$:

$$\sigma_t^{0r}(s(t), t) + \sigma^{1r}(s(t), t) = C_t^{0r}(s(t), t).$$

Using (3.7) and the total derivative of (2.7) in the above, we obtain

$$(3.8) \quad \sigma^{1r}(s(t), t) = -\dot{s}C_x^{0r}(s(t), t).$$

Substituting (3.7) and (3.8) into (2.17), we have, to leading order,

$$(3.9) \quad C_x^g(s(t), t) - D_r C_x^{0r}(s(t), t) = a\dot{s}.$$

Note that the behavior of the stress causes the form of (3.9) to be similar to the front condition for a standard Stefan problem. Although one may be tempted to introduce similarity variables at this stage due to the form of (3.9), this will not work, as shown in section 4.

Alternatively, we employ an integral method developed by Boley [26] for more standard diffusion problems. Edwards has used this method quite successfully to obtain solutions for polymer-penetrant systems governed by equations similar to (2.1a) and (2.1b) [15], [17], [19]. We assume that (3.2a), which holds for C^{0r} in the rubbery region $x > s(t)$, holds for some related function in the *entire* semi-infinite domain. We impose a *fictitious* Dirichlet boundary condition at $x = 0$ involving an unknown function $f^b(t)$. After requiring it to satisfy all the true front and initial conditions, this related function, restricted to the proper region of validity $x > s(t)$, will yield the solution C^{0r} we seek. Therefore, we let

$$(3.10a) \quad C^{0r}(x, t) = 1 - T^r(x, t), \quad x > s(t),$$

in which case (3.2a) and (3.3) become the following:

$$(3.10b) \quad T_t^r = D_r T_{xx}^r, \quad x > 0, \quad t > 0,$$

$$(3.11) \quad T^r(x, 0) = 0.$$

In addition, we have the fictitious boundary condition replacing (3.5):

$$(3.12) \quad T^r(0, t) = f^b(t).$$

The solution of (3.10b)–(3.12) is given by

$$T^r(x, t) = \frac{x}{2\sqrt{D_r\pi}} \int_0^t \frac{f^b(z)}{(t-z)^{3/2}} \exp\left[-\frac{x^2}{4D_r(t-z)}\right] dz,$$

from which we have

$$(3.13) \quad C^{0r}(x, t) = 1 - \frac{x}{2\sqrt{D_r\pi}} \int_0^t \frac{f^b(z)}{(t-z)^{3/2}} \exp\left[-\frac{x^2}{4D_r(t-z)}\right] dz, \quad x \geq s(t).$$

Substituting (3.13) into (2.7), we obtain the first condition relating s and f^b :

$$(3.14) \quad C_* = 1 - \frac{s}{2\sqrt{D_r\pi}} \int_0^t \frac{f^b(z)}{(t-z)^{3/2}} \exp\left[-\frac{s^2}{4D_r(t-z)}\right] dz.$$

4. The glassy region. To construct solutions in the glassy region, we let

$$(4.1) \quad C^g(x, t) \sim C^{0g}(x, t) + o(\epsilon), \quad \sigma^g(x, t) \sim \sigma^{0g}(x, t) + o(1)$$

in (2.14), (2.15), (2.18b), and (3.9), which yields, to leading orders,

$$(4.2a) \quad C_{tt}^{0g} = C_{xxt}^{0g} - C_t^{0g}, \quad 0 < x < s(t), \quad t > 0,$$

$$(4.2b) \quad \sigma_t^{0g} + \sigma^{0g} = C_t^{0g},$$

$$(4.3) \quad \sigma_{tt}^{0g} = \sigma_{xxt}^{0g} - \sigma_t^{0g},$$

$$(4.4) \quad D_0 \epsilon C_x^{0g}(0, t) + \sigma_x^{0g}(0, t) = k_0 \epsilon^{-1} [C^{0g}(0, t) - C_{\text{ext}}],$$

$$(4.5) \quad C_x^{0g}(s(t), t) - D_r C_x^{0r}(s(t), t) = a\dot{s}.$$

If $\sigma^{0g}(s(t), t) \neq 0$, we see from (2.8) that an interior layer is necessary around $x = s(t)$, since σ^{0g} is an order of magnitude larger than σ^{1r} . However, since the coefficient of the highest derivative in (4.2a) and (4.3) is at least as large as the coefficients of the other terms, there can be no $O(1)$ boundary or interior layers anywhere. Thus, we have that

$$(4.6) \quad \sigma^{0g}(s(t), t) = 0.$$

Integrating (4.2a) once with respect to t using (2.6), we have the following:

$$(4.7) \quad C_t^{0g} = C_{xx}^{0g} - C^{0g} + C_{\text{ext}}.$$

Using the integral method in this region, we let

$$(4.8) \quad C^{0g} = C_{\text{ext}} + e^{-t} T^g, \quad 0 < x < s(t),$$

in (4.7) and the leading order of (4.4), which yields

$$(4.9) \quad T_t^g = T_{xx}^g,$$

$$(4.10a) \quad T^g(0, t) = 0.$$

As in our construction of T^r , we impose a fictitious condition on the problem. This time the condition is at $t = 0$ and replaces (2.4a):

$$(4.10b) \quad T^g(x, 0) = f^i(x).$$

The e^{-t} term in (4.8) is the reason why a simple similarity-variable approach will not work for this problem and hence why the entire integral-method approach is necessary.

The solution to (4.9) and (4.10) is the following:

$$T^g(x, t) = \frac{1}{2\sqrt{\pi t}} \int_0^\infty f^i(z) \left\{ \exp\left[-\frac{(x-z)^2}{4t}\right] - \exp\left[-\frac{(x+z)^2}{4t}\right] \right\} dz,$$

from which we have

$$(4.11) \quad C^{0g}(x, t) = C_{\text{ext}} + \frac{e^{-t}}{2\sqrt{\pi t}} \int_0^\infty f^i(z) \left\{ \exp\left[-\frac{(x-z)^2}{4t}\right] - \exp\left[-\frac{(x+z)^2}{4t}\right] \right\} dz.$$

Substituting (4.11) into (2.7) gives us a condition relating s and f^i :

$$(4.12) \quad C_* - C_{\text{ext}} = \frac{e^{-t}}{2\sqrt{\pi t}} \int_0^\infty f^i(z) \left\{ \exp\left[-\frac{(s-z)^2}{4t}\right] - \exp\left[-\frac{(s+z)^2}{4t}\right] \right\} dz.$$

Last, using the derivatives of (3.13) and (4.11) in (3.9), we obtain

$$(4.13) \quad -\frac{e^{-t}}{4t^{3/2}\sqrt{\pi}} \int_0^\infty f^i(z) \left\{ (x-z) \exp\left[-\frac{(x-z)^2}{4t}\right] - (x+z) \exp\left[-\frac{(x+z)^2}{4t}\right] \right\} dz \\ + \frac{1}{2} \sqrt{\frac{D_r}{\pi}} \int_0^t \frac{f^b(z)}{(t-z)^{3/2}} \left[1 - \frac{s^2}{2D_r(t-z)} \right] \exp\left[-\frac{s^2}{4D_r(t-z)}\right] dz = as.$$

Equations (3.14), (4.12), and (4.13) provide three conditions on our three unknowns f^b , f^i , and s . In the following sections we shall construct asymptotic solutions of these equations.

To complete the solution of the problem, we must calculate the polymer network stress in the glassy region. To do so, we substitute (4.8) into (4.2b):

$$\sigma^{0g} + \sigma_t^{0g} = (e^{-t} T^g)_t,$$

from which we have

$$(4.14) \quad \sigma^{0g}(x, t) = e^{-t} \left[T^g(x, t) - T^g(x, s^{-1}(x)) - \int_{s^{-1}(x)}^t T^g(x, z) dz \right],$$

where $s^{-1}(x)$ is the inverse function defined by $s^{-1}(s(t)) = t$. Note that our solution (4.14) satisfies (4.6). It is clear that using the definition of T^g in (4.8) we could construct the value for $T^g(x, s^{-1}(x))$. However, to obtain an accurate solution it is convenient *not* to do so; the reasons for this will be more fully explained in the next section.

5. Small-time asymptotics. We first examine the solution for t near 0. For small t , the dominant contribution to the integral in (4.12) is from z near $s(t)$ and hence near 0. Thus, to construct the solution we write the leading orders of our unknowns in the following way:

$$(5.1a) \quad f^i(x) = f_0^i + o(1), \quad x \rightarrow 0,$$

$$(5.1b) \quad f^b(t) = f_0^b + o(1), \quad s = 2s_0 t^n + o(t^n), \quad n \geq 0, \quad t \rightarrow 0.$$

Making these substitutions into (4.12), (3.14), and (4.13), we have

$$(5.2) \quad C_{\text{ext}} + f_0^i e^{-t} \text{erf}(s_0 t^{n-1/2}) = C_*,$$

$$(5.3) \quad 1 - f_0^b \text{erfc}(s_0 t^{n-1/2} / \sqrt{D_r}) = C_*,$$

$$(5.4) \quad \frac{f_0^i e^{-t}}{\sqrt{\pi t}} \exp(-s_0^2 t^{2n-1}) - \frac{D_r f_0^b}{\sqrt{\pi D_r t}} \exp(-s_0^2 t^{2n-1}/D_r) = a \dot{s}.$$

If $n > 1/2$, we see from (5.2) that we have $C_{\text{ext}} = C_*$ to leading order, which is false. If $n < 1/2$, the leading order of (5.3) becomes $C_* = 1$, which is a vacuous case. Therefore, we conclude that $n = 1/2$, in which case the leading order of the expansion of (5.2) in t is

$$(5.5) \quad f_0^i = \frac{C_* - C_{\text{ext}}}{\text{erf } s_0},$$

while the leading order of the expansion of (5.3) in t is the following:

$$(5.6) \quad f_0^b = \frac{1 - C_*}{\text{erfc}(s_0/\sqrt{D_r})}.$$

Note that due to the forms of (3.13) and (4.11) we solve the boundary condition exactly, although we solve the front condition asymptotically.

Equation (5.4) becomes, to leading order in t ,

$$(5.7) \quad \frac{f_0^i}{\sqrt{\pi t}} \exp(-s_0^2) - f_0^b \sqrt{\frac{D_r}{\pi t}} \exp(-s_0^2/D_r) = \frac{a s_0}{\sqrt{t}}.$$

Substituting (5.5) and (5.6) into (5.7), we have the following:

$$(5.8) \quad g(s_0) \equiv \frac{(C_* - C_{\text{ext}}) \exp(-s_0^2)}{\text{erf } s_0} - \frac{(1 - C_*) \exp(-s_0^2/D_r) \sqrt{D_r}}{\text{erfc}(s_0/\sqrt{D_r})} = a s_0 \sqrt{\pi}.$$

The limiting behavior of $g(s_0)$ is

$$(5.9) \quad g(s_0) \sim \frac{(C_* - C_{\text{ext}}) \sqrt{\pi}}{2s_0} \text{ as } s_0 \rightarrow 0^+, \quad g(s_0) \sim -(1 - C_*) s_0 \sqrt{\pi} \text{ as } s_0 \rightarrow \infty.$$

Therefore, any line with slope greater than $-(1 - C_*) \sqrt{\pi}$ will intersect $g(s_0)$ for some $s_0 > 0$, producing a positive root of equation (5.8). Indeed, a line with such a slope satisfies

$$(5.10) \quad a > C_* - 1$$

as required by (2.13).

Graphs of (5.8) are shown in Fig. 5.1. Here the values of D_r and C_{ext} have been frozen and the values of C_* and a allowed to vary. The intersection of two curves denotes the value of s_0 which solves (5.8). Note that as C_* increases so does s_0 . This is because not as much penetrant needs to desorb for the solution to attain C_* at the front, and hence the front moves faster. As $C_* \rightarrow C_{\text{ext}}$, the intersection point s_0 moves to zero, which corresponds to the aforementioned case that $n > 1/2$. Also, as a decreases it takes less flux move to the front along, so the front will move faster, and hence s_0 increases.

We may rewrite (5.8) to obtain

$$(5.11) \quad \frac{(C_* - C_{\text{ext}}) \exp(-s_0^2)}{\text{erf } s_0} - a s_0 \sqrt{\pi} = \frac{(1 - C_*) \exp(-s_0^2/D_r) \sqrt{D_r}}{\text{erfc}(s_0/\sqrt{D_r})},$$

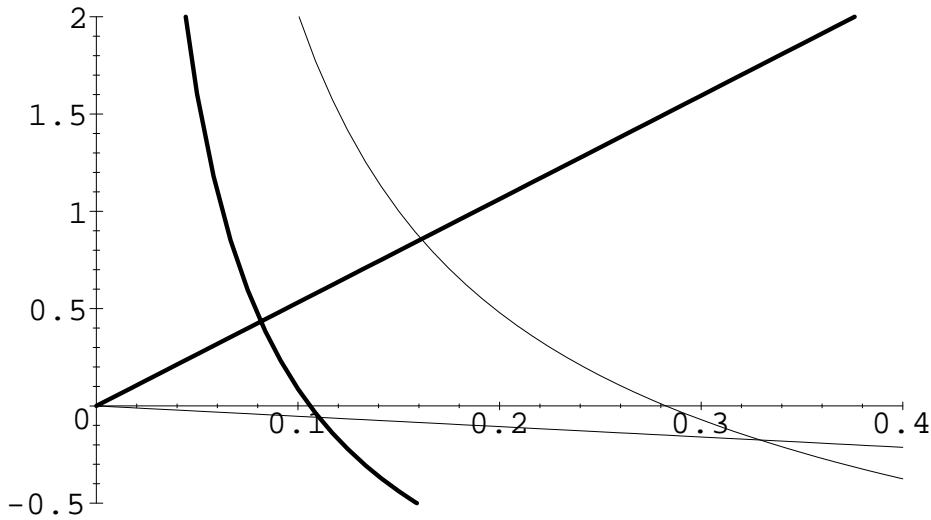


FIG. 5.1. Graphs of (5.8) for $D_r = 7, C_{\text{ext}} = 1/3$. Thick lines: $C_* = 1/2, a = 3$. Thin lines: $C_* = 2/3, a = -0.3$.

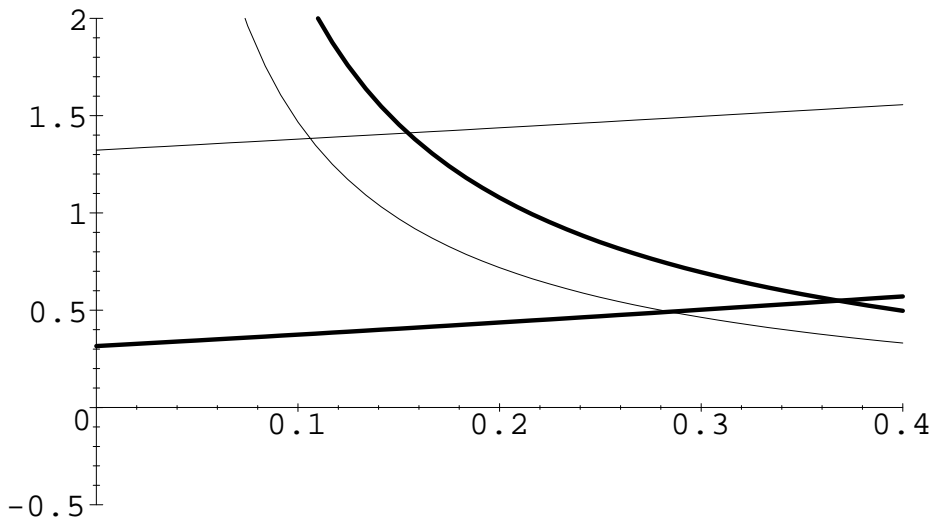


FIG. 5.2. Graphs of (5.11) for $a = 0, C_* = 1/2$. Thick lines: $D_r = 0.4, C_{\text{ext}} = 1/4$. Thin lines: $D_r = 7, C_{\text{ext}} = 1/3$.

graphs of which are shown in Fig. 5.2. Here the values of C_* and a have been frozen and the values of D_r and C_{ext} have been allowed to vary. Note that as D_r increases s_0 decreases; this is because the flux into the front from the rubbery region is larger and hence there is a greater barrier to surmount to propagate the front. Note also that as C_{ext} increases s_0 decreases. This is because the flux out of the front to the glassy region is smaller, and so we have the same situation as before.

Summarizing our results, we have the following:

$$t \rightarrow 0, \quad x \rightarrow 0,$$

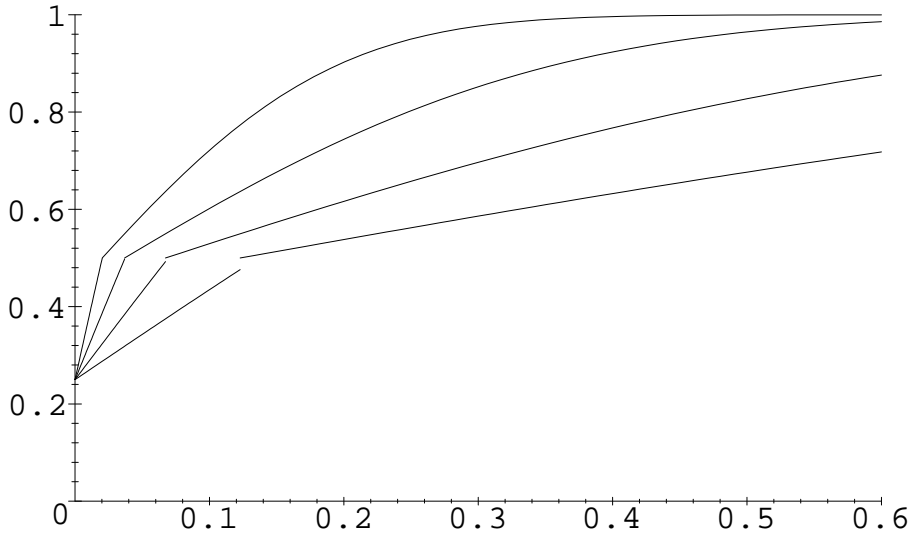


FIG. 5.3. $C^0(x, t)$ versus x for $a = 0$, $C_* = 1/2$, $D_r = 4$, $C_{\text{ext}} = 1/4$, $t = 0.0027, 0.009, 0.03$, and 0.1 .

$$(5.12) \quad s(t) \sim 2s_0\sqrt{t}, \quad \frac{(C_* - C_{\text{ext}}) \exp(-s_0^2)}{\text{erf } s_0} - \frac{(1 - C_*) \exp(-s_0^2/D_r)\sqrt{D_r}}{\text{erfc}(s_0/\sqrt{D_r})} = as_0\sqrt{\pi},$$

$$(5.13a) \quad T^g(x, t) \sim \frac{C_* - C_{\text{ext}}}{\text{erf } s_0} \text{erf} \left(\frac{x}{2\sqrt{t}} \right),$$

$$(5.13b) \quad C^{0g}(x, t) \sim C_{\text{ext}} + e^{-t}T^g(x, t), \quad 0 < x < s(t),$$

$$(5.14) \quad C^{0r}(x, t) \sim 1 - \frac{1 - C_*}{\text{erfc}(s_0/\sqrt{D_r})} \text{erfc} \left(\frac{x}{2\sqrt{D_r t}} \right), \quad x > s(t).$$

Graphs of C^0 versus x for various values of t are shown in Fig. 5.3. The gaps in the graph are due to the fact that we are solving the front condition asymptotically. As t increases, the small-time solution becomes less accurate, causing more pronounced gaps. Note with our choice of a that the *total* flux is continuous across the front. However, since the flux involves two terms and changing diffusion coefficients, C_x is *not* continuous across the front. Since the memory effects have not yet had enough time to become dominant, for small time the profiles are qualitatively similar to those for Fickian diffusion.

To calculate the stress, we first note from (5.12) that

$$(5.15) \quad s^{-1}(x) \sim \frac{x^2}{4s_0^2}.$$

In addition, we note from (5.13a) that for small time we have calculated

$$(5.16a) \quad T^g(s(t), t) = C_* - C_{\text{ext}}$$

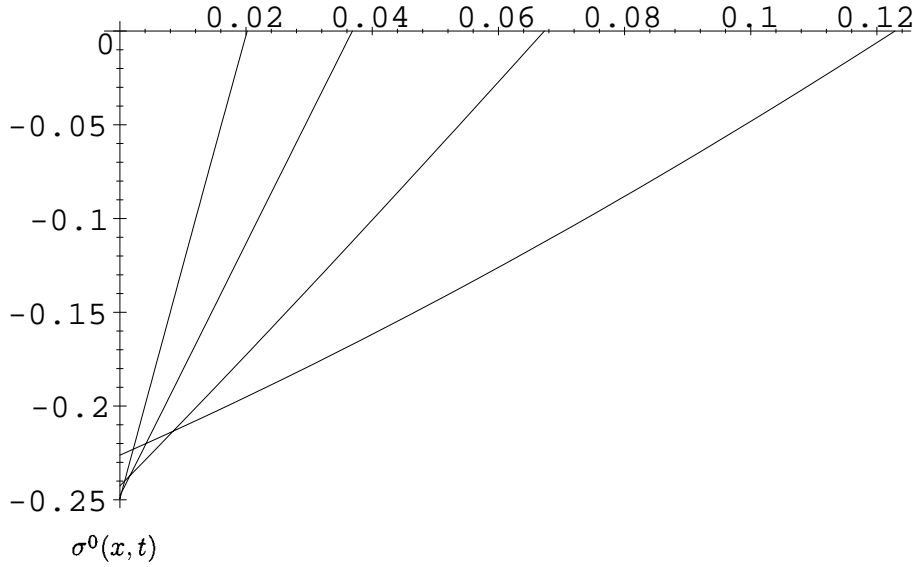


FIG. 5.4. $\sigma^0(x, t)$ versus x for $a = 0$, $C_* = 1/2$, $D_r = 4$, $C_{\text{ext}} = 1/4$, $t = 0.0027, 0.009, 0.03$, and 0.1 .

while from (4.8) we know that the exact value is

$$(5.16b) \quad T^g(s(t), t) = e^t (C_* - C_{\text{ext}}).$$

Of course, (5.16a) and (5.16b) are asymptotic to one another for small t . However, when calculating the stress, we use the calculated value (5.16a) in (4.14). That way, our stress will solve the boundary condition (4.6) exactly rather than asymptotically.

Substituting (5.13a), (5.15), and (5.16a) into (4.14), we have

$$(5.17) \quad \sigma^{0g}(x, t) = \frac{e^{-t}(C_* - C_{\text{ext}})}{\text{erf } s_0} \left[\text{erf} \left(\frac{x}{2\sqrt{t}} \right) \left(1 - t - \frac{x^2}{2} \right) - \left(1 - \frac{x^2}{4s_0^2} - \frac{x^2}{2} \right) \text{erf } s_0 - x\sqrt{\frac{t}{\pi}} \exp \left(-\frac{x^2}{4t} \right) + \frac{x^2}{2s_0\sqrt{\pi}} \exp(-s_0^2) \right].$$

Graphs of σ^0 versus x for various values of t are shown in Fig. 5.4. The choice of parameters is the same as in Fig. 5.3. Since $\sigma^r \equiv 0$ the polymer network stress in the rubbery region is not plotted. There are no gaps at $x = s(t)$ since we used (5.16a) to satisfy the front condition exactly. We note that we have a negative (compressive) stress in the polymer entanglement network since it wants to shrink as it dries out. Because most of the other studies of this model involved sorption experiments, this is the first manifestation of a negative polymer network stress that we have encountered.

6. Large-time asymptotics. Next we look at the solution for $t \rightarrow \infty$. Due to the form of the operator in (4.7), to satisfy (4.12) the contribution from the integral must be *exponentially* large as $t \rightarrow \infty$. Therefore, we expect $f^i(x)$ to be exponentially large as well. Following our work in [17], to obtain this behavior we assume the following functional form for $f^i(x)$:

$$(6.1) \quad f^i(x) \sim f_\infty^i e^{A_i x}, \quad x \rightarrow \infty.$$

Substituting (6.1) into (4.11), we have

$$(6.2) \quad C^{0g} \sim C_{\text{ext}} + \frac{f_{\infty}^i}{2} \exp [(A_i^2 - 1)t] \times \left[e^{A_i x} \operatorname{erfc} \left(-\frac{x}{2\sqrt{t}} - A_i \sqrt{t} \right) - e^{-A_i x} \operatorname{erfc} \left(\frac{x}{2\sqrt{t}} - A_i \sqrt{t} \right) \right].$$

However, we note from (6.2) that the only form for s which will cause our function to remain bounded as $t \rightarrow \infty$ is one which is proportional to t . Therefore, we let

$$(6.3) \quad s(t) \sim 2s_{\infty}t.$$

Substituting (6.2) and (6.3) into (2.7) and solving, we obtain

$$(6.4) \quad A_i = -s_{\infty} + \sqrt{s_{\infty}^2 + 1}, \quad f_{\infty}^i = C_* - C_{\text{ext}},$$

but at this stage s_{∞} is still undetermined. We note that $A_i^2 < 1$.

To maintain a constant value as $t \rightarrow \infty$ with $s \propto t$, we see that f^b must diverge exponentially, so we have [17]

$$(6.5) \quad f^b(t) \sim f_{\infty}^b e^{A_b^2 t},$$

from which (3.13) becomes

$$(6.6) \quad C^{0r}(x, t) = 1 - \frac{f_{\infty}^b}{2} e^{A_b^2 t} \left[\exp \left(\frac{A_b x}{\sqrt{D_r}} \right) \operatorname{erfc} \left(\frac{x}{2\sqrt{D_r t}} + A_b \sqrt{t} \right) + \exp \left(-\frac{A_b x}{\sqrt{D_r}} \right) \operatorname{erfc} \left(\frac{x}{2\sqrt{D_r t}} - A_b \sqrt{t} \right) \right].$$

Asymptotically expanding (6.6) for large t (using our assumption for s) and substituting the result into (2.7), we have

$$(6.7) \quad \frac{f_{\infty}^b}{2} \left\{ \frac{\exp(-s_{\infty}^2 t / D_r)}{(s_{\infty} / \sqrt{D_r} + A_b) \sqrt{\pi t}} + \exp \left[(A_b^2 - 2A_b s_{\infty} / \sqrt{D_r}) t \right] \operatorname{erfc} \left[(s_{\infty} / \sqrt{D_r} - A_b) \sqrt{t} \right] \right\} = 1 - C_*,$$

from which we have the following:

$$(6.8) \quad f_{\infty}^b = 1 - C_*, \quad A_b = 2s_{\infty} / \sqrt{D_r}.$$

To solve for s_{∞} , we substitute our results given by (6.1), (6.3)–(6.5), and (6.8) into (4.13). The only terms which are not exponentially decaying for $s \propto t$ for large t are the derivatives of the exponentials $e^{-A_b x / \sqrt{D_r}}$ and $e^{A_i x}$. Keeping that in mind, we see that the leading order of (4.13) is given by

$$(6.9) \quad \frac{A_i f_{\infty}^i}{2} \exp [(A_i^2 - 1)t + A_i s] \operatorname{erfc} \left(-\frac{s}{2\sqrt{t}} - A_i \sqrt{t} \right) - \frac{f_{\infty}^b A_b \sqrt{D_r}}{2} \exp \left(A_b^2 t - A_b s / \sqrt{D_r} \right) \operatorname{erfc} \left(\frac{s}{2\sqrt{D_r t}} - A_b \sqrt{t} \right) = a s.$$

Substituting (6.3), (6.4), and (6.8) into (6.9) and expanding for large t , we have

$$(6.10a) \quad s_\infty = \frac{C_* - C_{\text{ext}}}{2\sqrt{(a+1 - C_{\text{ext}})(a+1 - C_*)}}.$$

Since $C_* > C_{\text{ext}}$, s_∞ is real whenever

$$(6.10b) \quad a > C_* - 1,$$

as required by (2.13).

Summarizing our results, we have the following:

$$t \rightarrow \infty, \quad x \rightarrow \infty,$$

$$(6.11) \quad s(t) \sim 2s_\infty t, \quad s_\infty = \frac{C_* - C_{\text{ext}}}{2\sqrt{(a+1 - C_{\text{ext}})(a+1 - C_*)}},$$

$$(6.12a) \quad T^g(x, t) \sim \frac{(C_* - C_{\text{ext}})e^{A_i^2 t}}{2} \left[e^{A_i x} \operatorname{erfc} \left(-\frac{x}{2\sqrt{t}} - A_i \sqrt{t} \right) - e^{-A_i x} \operatorname{erfc} \left(\frac{x}{2\sqrt{t}} - A_i \sqrt{t} \right) \right],$$

$$(6.12b) \quad A_i = -s_\infty + \sqrt{s_\infty^2 + 1},$$

$$(6.12c) \quad C^{0g}(x, t) \sim C_{\text{ext}} + e^{-t} T^g(x, t), \quad 0 < x < s(t),$$

$$(6.13) \quad C^{0r}(x, t) = 1 - \frac{1 - C_*}{2} e^{4s_\infty^2 t / D_r} \left[\exp \left(\frac{2xs_\infty}{D_r} \right) \operatorname{erfc} \left(\frac{x}{2\sqrt{D_r t}} + 2s_\infty \sqrt{\frac{t}{D_r}} \right) + \exp \left(-\frac{2xs_\infty}{D_r} \right) \operatorname{erfc} \left(\frac{x}{2\sqrt{D_r t}} - 2s_\infty \sqrt{\frac{t}{D_r}} \right) \right], \quad x > s(t).$$

Graphs of C^0 versus x for the same parameters as in section 5 and various values of t are shown in Fig. 6.1. Once again, there are gaps in the graph in the region where our asymptotics begin to lose validity. Note the development of the glassy skin where the concentration in the polymer is nearly identical to that in the external environment. These profiles are similar to those in [20] if we take the special case $C_{\text{ext}} = 0$.

Although the profiles in the glassy region are reminiscent of constant solutions matched through an interior layer to another value, no such layer exists. Rather, the transition is sharp due to the presence of e^{-t} in the expression for C^{0g} . Unless we are very near the front (where the growing exponential in $f^i(x)$ dominates), the concentration is transcendently close to C_{ext} . Note that the expression for C^{0g} given by (5.13b) is also transcendently close to C_{ext} for large time. Therefore, since the two expressions for the solution are transcendently close, we have used (6.12c) to graph C^{0g} for the *entire* glassy region, not just for $x \rightarrow \infty$.

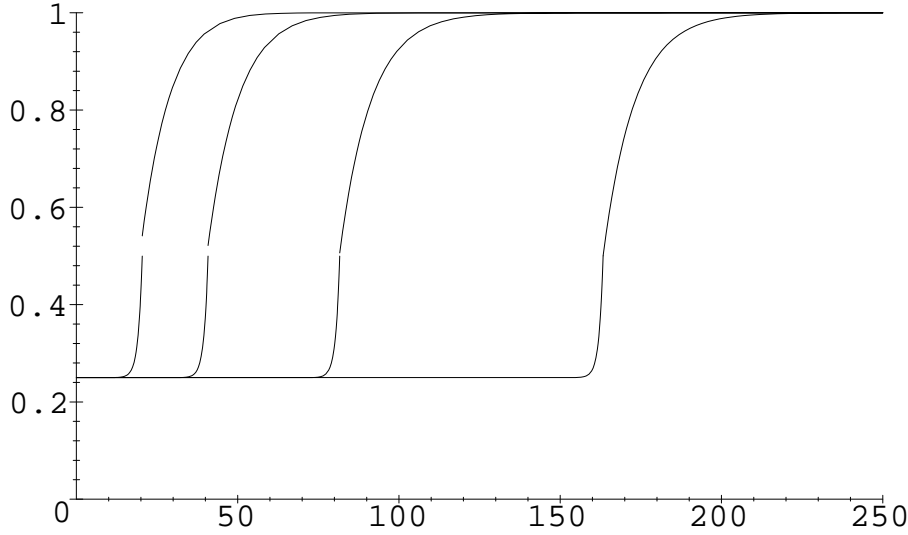


FIG. 6.1. $C^0(x, t)$ versus x for $a = 0$, $C_* = 1/2$, $D_r = 4$, $C_{\text{ext}} = 1/4$, $t = 50, 100, 200, 400$.

To calculate σ^{0g} , we first note from (6.11) that

$$(6.14) \quad s^{-1}(x) \sim \frac{x}{2s_\infty}.$$

We again use the calculated rather than the actual value for $T^g(s(t), t)$. Hence, substituting (6.12a) and (6.14) into (4.14), we have

$$(6.15) \quad \begin{aligned} \sigma^{0g}(x, t) = & \frac{e^{-t}(C_* - C_{\text{ext}})}{2} \left(\left(1 - \frac{1}{A_i^2} \right) \left\{ e^{A_i^2 t} \left[e^{A_i x} \operatorname{erfc} \left(-\frac{x}{2\sqrt{t}} - A_i \sqrt{t} \right) \right. \right. \right. \\ & - \left. \left. \left. e^{-A_i x} \operatorname{erfc} \left(\frac{x}{2\sqrt{t}} - A_i \sqrt{t} \right) \right] - e^{A_i^2 x / 2s_\infty} \left[e^{A_i x} \operatorname{erfc} \left(-\sqrt{\frac{x(s_\infty^2 + 1)}{2s_\infty}} \right) \right. \right. \right. \\ & - \left. \left. \left. e^{-A_i x} \operatorname{erfc} \left(\sqrt{\frac{x s_\infty}{2}} - A_i \sqrt{\frac{x}{2s_\infty}} \right) \right] \right\} - \frac{2}{A_i^2} \left[\operatorname{erfc} \left(\frac{x}{2\sqrt{t}} \right) \right. \right. \\ & \left. \left. - \operatorname{erfc} \left(\sqrt{\frac{x s_\infty}{2}} \right) \right] \right). \end{aligned}$$

Graphs of σ^0 versus x for various values of t are shown in Fig. 6.2. The parameters used are the same as those in section 5. Once again, we have a negative (compressive) stress in the polymer network. Note from (4.14) that to have an expression for the stress that is valid away from the front, we must integrate over a time history where we have not constructed an expansion. Therefore, our expression (6.15) is valid only for a narrow region near the front and thus the plotted values of the graph away from the front should be suspect.

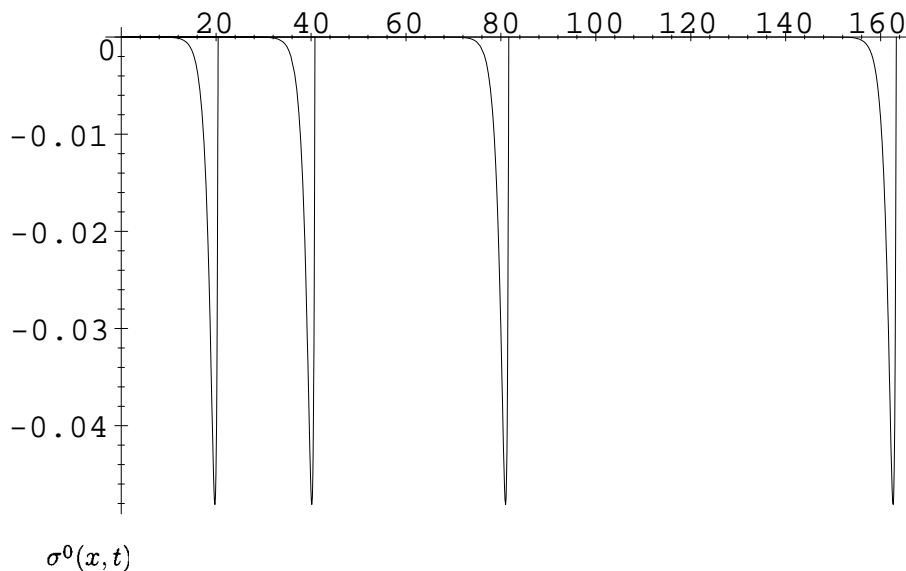


FIG. 6.2. $\sigma^0(x, t)$ versus x for $a = 0$, $C_* = 1/2$, $D_r = 4$, $C_{\text{ext}} = 1/4$, $t = 50, 100, 200, 400$.

We note that for large t the magnitude of the stress attains a maximum value *behind* the glass-rubber interface. Thus for large time the stress builds up in the glassy region before being released near the glass-rubber interface as a result of the disentangling of the polymer network. Contrast this with the monotonic behavior of the stress for small time. This type of behavior has been seen previously in this model in sorption studies [17].

7. Some remarks on trapping skinning. To examine whether trapping skinning occurs, we define the accumulated flux F through the exposed boundary:

$$(7.1) \quad F \equiv \int_0^\infty [D(C)C_x + \sigma_x](0, t) dt.$$

From (2.5), we see that the driving force for the desorption can be enhanced by increasing k or reducing C_{ext} . To leading order, adjusting k does nothing to affect the problem since k is already $O(\epsilon^{-1})$. Therefore, we examine the effects of varying C_{ext} .

We begin with the case where $C_{\text{ext}} > C_*$. Since the polymer is always in the rubbery region, we may substitute (3.4) into (7.1), which yields, to leading order,

$$(7.2) \quad F = D_r \int_0^\infty C_x^{0r}(0, t) dt.$$

Substituting (3.6) into (7.2), we have the following:

$$(7.3) \quad F = 2(1 - C_{\text{ext}}) \sqrt{\frac{D_r}{\pi}} \lim_{t \rightarrow \infty} \sqrt{t}.$$

Since the polymer is taken to be semi-infinite, an infinite amount of penetrant is desorbed. However, if we run the experiment to a large but finite time $t_>$, we see that decreasing C_{ext} will increase F , as expected.

If $C_{\text{ext}} < C_*$, the polymer at the exposed boundary is always glassy. Substituting our expression for D_g into (7.1), we obtain, to leading order,

$$(7.4) \quad F = \int_0^\infty \sigma_x^{0g}(0, t) dt.$$

Unfortunately, due to the nature of the problem, we are unable to find a closed-form solution for F . To obtain such a solution, a full numerical study would have to be employed. However, using heuristic reasoning, we can provide strong evidence that leads us to believe that F is finite.

From considerations of the flux motivated by the form of (4.4), we have that

$$(7.5) \quad \sigma_x^{0g}(0, t) \geq 0.$$

Taking the derivative of (4.2b) with respect to x , we have the following:

$$\sigma_{xt}^{0g} + \sigma_x^{0g} = C_{xt}^{0g}.$$

Substituting (7.5) into the above evaluated at the exposed surface yields

$$(7.6) \quad \sigma_{xt}^{0g}(0, t) \leq C_{xt}^{0g}(0, t).$$

To compute the relative sizes of the stress and concentration gradients at the exposed surface, we examine our solutions for small time. Taking the derivative of (5.13b) with respect to x at $x = 0$, we have

$$(7.7a) \quad C_x^{0g}(0, t) \sim \frac{(C_* - C_{\text{ext}})e^{-t}}{\sqrt{\pi t} \operatorname{erf} s_0}.$$

Taking the derivative of (5.17) with respect to x at $x = 0$, we have the following:

$$(7.7b) \quad \sigma_x^{0g}(0, t) = \frac{e^{-t}(C_* - C_{\text{ext}})(1 - 2t)}{\operatorname{erf} s_0 \sqrt{\pi t}}.$$

Therefore, for small t , we have

$$(7.8) \quad \sigma_x^{0g}(0, t) \leq C_x^{0g}(0, t).$$

However, since (7.6) holds for all time, (7.8) holds for all time as well. Hence (7.4) may be written as

$$(7.9) \quad F \leq F_{<} + F_m + F_{>},$$

$$(7.10a) \quad F_{<} = \int_0^{t_{<}} C_x^{0g}(0, t) dt, \quad t_{<} \ll 1,$$

$$F_m = \int_{t_{<}}^{t_{>}} C_x^{0g}(0, t) dt, \quad t_{>} \gg 1,$$

$$(7.10b) \quad F_{>} = \int_{t_{>}}^\infty C_x^{0g}(0, t) dt.$$

It is straightforward to compute the integral in (7.10a) using (7.7a):

$$(7.11) \quad F_{<} = \frac{(C_* - C_{\text{ext}}) \operatorname{erf}(\sqrt{t_{<}})}{\operatorname{erf} s_0}.$$

Since the interval of integration for F_m is finite, F_m must be finite unless the integrand diverges, which we do not expect to happen, both on physical grounds and due to the nature of the operator in (4.7). To estimate $F_{>}$, we take the derivative of (6.12c) with respect to x at $x = 0$ and expand for large t :

$$(7.12) \quad C_x^{0g}(0, t) = 2A_i(C_* - C_{\text{ext}})e^{(A_i^2-1)t}.$$

From our work in section 6 we know that $A_i^2 < 1$, and hence we have that this term, although larger than (7.7a) for large t , still decays exponentially.

We cannot compute $F_{>}$ directly, since neither (7.7a) nor (7.12) is technically in its region of validity. However, we do know that the operator in (4.7) has an inherent e^{-t} decay in it, as evidenced by the form of (4.8). Hence, our fictitious initial condition f^i had to grow exponentially as $x \rightarrow \infty$ for there to be an $O(1)$ value of the concentration at the front. Since there are no other mechanisms for decay in the problem, we see that the exponential form of f^i given in (6.1) is a correct order-of-magnitude estimate for the fictitious initial condition in the entire interval $x > 0$.

Therefore, we use (7.12) as an estimate for the integrand in $F_{>}$, which yields

$$(7.13) \quad F_{>} \approx \frac{2A_i(C_* - C_{\text{ext}})e^{(A_i^2-1)t_{>}}}{1 - A_i^2}.$$

Using (7.11), (7.13), and our knowledge about F_m , we deduce that F is bounded. Note that since (7.12) is larger than (7.7a), using (7.7a) as an approximation to the integrand would still lead to a finite value for F .

Although the reasoning in this section is heuristic, it does provide strong evidence showing that F is finite when $C_{\text{ext}} < C_*$. If this is indeed the case, decreasing C_{ext} (and hence increasing the driving force) has reduced the flux desorbed from an infinite to a finite quantity. Therefore, we believe that the polymer system we are modeling does exhibit trapping skinning. This is directly due to the exponential decay inherent in (4.7).

8. Conclusions. During the desorption of saturated polymers, several anomalous features can appear. First, a glassy skin can form at the exposed surface. Since the molecular diffusion coefficient is smaller in the glassy region [1], [2], [3], the formation of such a skin slows desorption [7]. In extreme cases, trapping skinning can occur, and an increase in the driving force will decrease the total flux through the exposed surface. The lower diffusion coefficient in the glassy skin is not adequate to describe such behavior; rather, nonlinear viscoelastic effects must also be considered [2], [3], [10].

The mathematical model presented has captured this behavior in a previous study [20], but the analysis held only for dry environments where $C_{\text{ext}} = 0$. Since “humid” environments where $C_{\text{ext}} \neq 0$ are also of interest, in this work we formulated combinations of parameters that allowed the solutions to be valid for diffusion into both dry and “humid” environments. The ensuing model, which contains memory effects, leads to a set of coupled partial differential equations for the stress and concentration of penetrant in the polymer network.

Due to the large value of k , which represents a highly permeable interface, the state of the polymer at the exposed surface is directly determined by C_{ext} . If $C_{\text{ext}} \geq C_*$, the polymer is always rubbery, and the resulting problem could be solved in closed form. The solution behaves in a purely Fickian way since memory effects are negligible in the rubbery state [5]. Due to the Fickian nature of the operator and the infinite extent of the polymer, the accumulated flux through the exposed surface diverges like $t^{1/2}$.

A more complicated case ensues when $C_{\text{ext}} \leq C_*$. In this case there is an instantaneous change in the polymer from rubber to glass at the exposed surface. The resulting moving boundary-value problem couples two different operators on each side of the interface. This situation, which is much more complicated than a standard Stefan problem, is not solvable by similarity solutions. Therefore, we employed an integral method pioneered by Boley [26] to obtain asymptotic solutions.

The glass-rubber interface initially moves like $t^{1/2}$, as is standard in a purely Fickian problem, since the memory has not had time to develop. However, as time progresses, the front moves with constant speed—behavior which is reminiscent of case II diffusion in sorption experiments [27]. Since the underlying nature of the operator in the glassy region has an exponential decay in time, we were able to provide strong evidence that the accumulated flux is finite for this case. Since decreasing C_{ext} corresponds to increasing the driving force, we see that this phenomenon corresponds to trapping skinning.

9. Nomenclature.

9.1. Variables and parameters. Units are listed in terms of length (L), mass (M), moles (N), or time (T). The equation number where a particular quantity first appears is listed, if applicable.

- A : constant, variously defined (6.1).
- a : coefficient in flux-front speed relationship (2.9).
- $C(x, t)$: concentration of penetrant at position x and time t (2.1a).
- $D(C)$: molecular diffusion coefficient for system (2.1a).
- F : accumulated flux through the exposed surface (7.1).
- $f(\cdot)$: fictitious boundary condition for T (3.12).
- $g(s_0)$: function whose roots yield the coefficient of the short-time front position (5.8).
- $J(x, t)$: flux at position x and time t .
- k : measure of permeability of outer boundary (2.5).
- n : variable exponent for small-time asymptotics (5.1b).
- $s(t)$: position of glass-rubber interface, defined by $C(s(t), t) = C_*$ (2.7).
- $s^{-1}(x)$: inverse function of $s(t)$, defined by $s^{-1}(s(t)) = t$ (4.14).
- T : embedding of C from one region to the fully semi-infinite region (3.10a).
- t : time from beginning of experiment (2.1a).
- x : distance from boundary (2.1a).
- \mathcal{Z} : the integers.
- z : dummy integration variable.
- α : dimensionless parameter, value $1 + D_r$ (2.16a).
- $\beta(C)$: inverse of the relaxation time, units T^{-1} (2.1b).
- γ : dimensionless parameter, value $\mu_0/\nu\beta_g$ (2.14a).
- ϵ : perturbation expansion parameter, value β_g/β_r .
- μ : coefficient of concentration in stress evolution equation, units ML^2/NT^3 (2.1b).

ν : normalization factor for σ , units ML^2/NT^2 (2.1b).
 $\sigma(x, t)$: stress in polymer entanglement network at position x and time t (2.1a).

9.2. Other notation.

b : as a superscript, used to indicate a quantity at $x = 0$.
 ext: as a subscript, used to indicate a value exterior to the polymer (2.5).
 g : as a sub- or superscript, used to indicate the glassy state (2.1b).
 i : as a sub- or superscript, used to indicate a quantity at $t = 0$ (2.4b).
 $j \in \mathcal{Z}$: as a sub- or superscript, used to indicate a term in an expansion, either in t or ϵ .
 m : as a subscript, used to indicate a moderate time (7.9).
 r : as a sub- or superscript, used to indicate the rubbery state (2.2).
 $\dot{\cdot}$: used to indicate differentiation with respect to t (2.9).
 $*$: as a subscript, used to indicate a quantity at the transition value between the glassy and rubbery states (2.2).
 $>$: as a subscript, used to indicate a large time.
 ∞ : as a subscript, used to indicate a term in an expansion for large t (6.1).
 $<$: as a subscript, used to indicate a small time (7.9).
 $[\cdot]_s$: jump across the front s , defined as $\cdot^g(s^-(t), t) - \cdot^r(s^+(t), t)$ (2.9).

Acknowledgments. The author wishes to thank Donald S. Cohen and Christopher Durning for their contributions, both direct and indirect, to this paper. Many of the calculations herein were performed using Maple.

REFERENCES

- [1] R. A. CAIRNCROSS, L. F. FRANCIS, AND L. E. SCRIVEN, *Competing drying and reaction mechanisms in the formation of sol-to-gel films, fibers, and spheres*, Drying Tech. J., 10 (1992), pp. 893–923.
- [2] R. A. CAIRNCROSS, L. F. FRANCIS, AND L. E. SCRIVEN, *Predicting drying in coatings that react and gel: Drying regime maps*, AIChE J., 42 (1996), pp. 55–67.
- [3] R. A. CAIRNCROSS AND C. J. DURNING, *A model for drying of viscoelastic coatings*, AIChE J., 42 (1996), pp. 2415–2425.
- [4] C. A. FINCH, ED., *Chemistry and Technology of Water-Soluble Polymers*, Plenum, New York, 1983.
- [5] W. R. VIETH, *Diffusion in and Through Polymers: Principles and Applications*, Oxford University Press, Oxford, UK, 1991.
- [6] J. S. VRENTAS, C. M. JORZELSKI, AND J. L. DUDA, *A Deborah number for diffusion in polymer-solvent systems*, AIChE J., 21 (1975), pp. 894–901.
- [7] G. W. POWERS AND J. R. COLLIER, *Experimental modelling of solvent-casting thin polymer films*, Polymer Engrg. Sci., 30 (1990), pp. 118–123.
- [8] D. H. CHARLESWORTH AND W. R. MARSHALL, JR., *Evaporation from drops containing dissolved solids*, AIChE J., 6 (1960), pp. 9–23.
- [9] J. E. ANDERSON AND R. ULLMAN, *Mathematical analysis of factors influencing the skin thickness of asymmetric reverse osmosis membranes*, J. Appl. Phys., 44 (1973), pp. 4303–4311.
- [10] J. CRANK, *The influence of concentration-dependent diffusion on rate of evaporation*, Proc. Phys. Soc., 63 (1950), pp. 484–491.
- [11] H. L. FRISCH, *Sorption and transport in glassy polymers—A review*, Polymer Engrg. Sci., 20 (1980), pp. 2–13.
- [12] D. R. PAUL AND W. J. KOROS, *Effect of partially immobilizing sorption on permeability and diffusion time lag*, J. Polymer Sci., 14 (1976), pp. 675–685.
- [13] W. R. VIETH AND K. J. SLADEK, *A model for diffusion in a glassy polymer*, J. Colloid Sci., 20 (1965), pp. 1014–1033.
- [14] J. CRANK, *The Mathematics of Diffusion*, 2nd ed., Clarendon Press, Oxford, UK, 1976.
- [15] D. A. EDWARDS AND D. S. COHEN, *A mathematical model of a dissolving polymer*, AIChE J., 41 (1995), pp. 2345–2355.

- [16] D. A. EDWARDS AND D. S. COHEN, *An unusual moving boundary condition arising in anomalous diffusion problems*, SIAM J. Appl. Math., 55 (1995), pp. 662–676.
- [17] D. A. EDWARDS, *Constant front speed in weakly diffusive non-Fickian systems*, SIAM J. Appl. Math., 55 (1995), pp. 1039–1058.
- [18] D. A. EDWARDS, *Non-Fickian diffusion in thin polymer films*, J. Polymer Sci. B: Polymer Phys., 34 (1996), pp. 981–997.
- [19] D. A. EDWARDS, *The effect of a varying diffusion coefficient in polymer-penetrant systems*, IMA J. Appl. Math., 55 (1995), pp. 49–66.
- [20] D. A. EDWARDS, *A mathematical model for trapping skinning in polymers*, Stud. Appl. Math., 99 (1997), pp. 49–80.
- [21] C. Y. HUI, K. C. WU, R. C. LASKY, AND E. J. KRAMER, *Case II diffusion in polymers, I: Transient swelling*, J. Appl. Phys., 61 (1987), pp. 5129–5136.
- [22] C. Y. HUI, K. C. WU, R. C. LASKY, AND E. J. KRAMER, *Case II diffusion in polymers, II: Steady state front motion*, J. Appl. Phys., 61 (1987), pp. 5137–5149.
- [23] J. CRANK, *Diffusion in media with variable properties, part III: Diffusion coefficients which vary discontinuously with concentration*, Trans. Farad. Soc., 47 (1951), pp. 450–461.
- [24] D. S. COHEN AND A. B. WHITE, JR., *Sharp fronts due to diffusion and stress at the glass transition in polymers*, J. Polymer Sci. B: Polymer Phys., 27 (1989), pp. 1731–1747.
- [25] W. G. KNAUSS AND V. H. KENNER, *On the hygrothermomechanical characterization of polyvinyl acetate*, J. Appl. Phys., 51 (1980), pp. 5131–5136.
- [26] B. A. BOLEY, *A method of heat conduction analysis of melting and solidification problems*, J. Math. Phys., 40 (1961), pp. 300–313.
- [27] N. THOMAS AND A. H. WINDLE, *Transport of methanol in poly-(methyl-methacrylate)*, Polymer, 19 (1978), pp. 255–265.